

Energy efficiency and area spectral efficiency tradeoff for coexisting wireless body sensor networks

Ruixia LIU^{1,2}, Yinglong WANG², Shangbin WU³,
Cheng-Xiang WANG^{3*} & Wensheng ZHANG⁴

¹College of Information Science and Engineering, Shandong University of Science and Technology, Qingdao 266590, China;

²Shandong Provincial Key Laboratory of Computer Network, Shandong Computer Science Center (National Supercomputer Center in Jinan), Jinan 250101, China;

³Institute of Sensors, Signals and Systems, School of Engineering and Physical Sciences, Heriot-Watt University, Edinburgh EH144AS, UK;

⁴Shandong Provincial Key Laboratory of Wireless Communication Technologies, School of Information Science and Engineering, Shandong University, Jinan 250100, China

Received June 13, 2016; accepted August 16, 2016; published online November 2, 2016

Abstract The coexistence of wireless body sensor networks (WBSNs) is a very challenging problem, due to strong interference, which seriously affects energy consumption and spectral reuse. The energy efficiency and spectral efficiency are two key performance evaluation metrics for wireless communication networks. In this paper, the fundamental tradeoff between energy efficiency and area spectral efficiency of WBSNs is first investigated under the Poisson point process (PPP) model and Matern hard-core point process (HCPP) model using stochastic geometry. The circuit power consumption is taken into consideration in energy efficiency calculation. The tradeoff judgement coefficient is developed and is shown to serve as a promising complementary measure. In addition, this paper proposes a new nearest neighbour distance power control strategy to improve energy efficiency. We show that there exists an optimal transmit power highly dependant on the density of WBSNs and the nearest neighbour distance. Some important properties are also addressed in the analysis of coexisting WBSNs based on the IEEE 802.15.4 standard, such as the impact of intensity nodes distribution, optimal guard zone, and outage probability. Simulation results show that the proposed power control design can reduce the outage probability and enhance energy efficiency. Energy efficiency and area spectral efficiency of the HCPP model are better than those of the PPP model. In addition, the optimal density of WBSNs coexistence is obtained.

Keywords WBSNs coexistence, stochastic geometry, energy efficiency, area spectral efficiency, power control

Citation Liu R X, Wang Y L, Wu S B, et al. Energy efficiency and area spectral efficiency tradeoff for coexisting wireless body sensor networks. *Sci China Inf Sci*, 2016, 59(12): 122311, doi: 10.1007/s11432-016-0320-1

1 Introduction

Population ageing is becoming a major problem in the modern society [1]. Wireless body sensor networks (WBSNs) for health monitoring systems are expected to play an important role on the aged care. WBSNs

*Corresponding author (email: Cheng-Xiang.Wang@hw.ac.uk)

have been devised for monitoring condition of the elderly and chronically ill people with a network of on-body sensors [1,2]. In many cases, there are often a group of people with wireless sensor nodes together in a small area, e.g., patients in hospitals or elderly people at nursing homes. The multi-WBSNs coexisting has a notable effect on the performance of networks [3]. Furthermore, both software and hardware resources are limited in WBSNs nodes. The node is supplied by battery so that its energy is limited. Besides, WBSNs based on the IEEE 802.15.4 standard operate in the license-free industrial, scientific, and medical (ISM) band. This is an overcrowded radio band which is shared with other major wireless standards such as IEEE 802.11, Bluetooth, and cordless phone [4]. There exist some challenges for the design of WBSNs owing to the very stringent application requirements such as power consumption, interference, reliability, latency, and bandwidth limitations, especially mobility or overlapped WBSNs.

How to efficiently design and manage the limited resources of wireless system has caught more and more attention. On one hand, energy consumption is a critical design issue for wireless sensor nodes, particularly for WBSNs. The devices are generally battery-powered and the battery lifetime is required to operate for months or even years. Improving the energy efficiency of WBSNs is generally the most important goal to support medical applications. On the other hand, most conventional performance metrics for wireless networks concerns spectrum utilization efficiency. It needs to minimize the number of frequency channels required to accommodate more networks. In many real scenarios where the density of nodes is reasonably high, the interference between nodes becomes a dominant factor affecting the overall networks performance [5]. It is therefore necessary to analyze the spectral efficiency of the coexisting WBSNs. The energy efficiency and spectral efficiency, which are conflicting, are becoming one of the key performance evaluation criteria for wireless communication. They can be linked together through their tradeoff.

Stochastic geometry is a powerful tool that has been used to model large-scale ad hoc wireless networks and to develop tractable models in the analysis and design of networks with random topologies [6]. It allows us to study the average behaviour over many spatial realizations of wireless networks [7]. There are various models for point processes in stochastic geometry. The simplest and most important random point pattern is the Poisson point process (PPP). This paper use stochastic geometry analysis to design a framework for coexisting WBSNs.

WBSNs have the opportunity of developing a large number of applications in several fields, including mobile health, aged care, sports and entertainments [8]. As shown in [9], a system was proposed which allowed patients to perform basic stroke rehabilitation including some wireless nodes (Node2s) and app software on iPhone or iPad. The authors of [10] described a home care system for elderly by four detached multi-sensor network. This network can detect heart rate and body movement. A novel wearable inertial sensor framework was proposed capable of automatically classifying symmetrical and asymmetrical running styles[11].

The main wireless communication standards considered in WBSNs are: IEEE 802.15.4 [12], IEEE 802.15.6 [13], and Bluetooth Low Energy [14]. Many papers [15–17] about IEEE 802.15.4 protocol are based on modeling, protocol analysis and protocol optimization. A Markov chain based analytical model was proposed in [15] to analyze performance of the slotted carrier sense multiple access with collision avoidance (CSMA/CA) mechanism in the IEEE 802.15.4 standard. This proposed accurate model considered about reliability, delay and energy consumption. In [16], the authors developed a novel framework to design spectrum-efficient multi-channel random wireless networks based on the IEEE 802.15.4 standard. An energy-efficient MAC protocol was designed in [17] to meet demands of sleeping medical emergency monitoring WBSNs.

IEEE 802.15.4 standard defines the protocol and compatible interconnection for data communication devices for low-rate, low-power, and low-cost short-range radio frequency (RF) transmissions in a wireless personal area network (WPAN). It uses two types of channel access mechanism: the beacon enabled and non-beacon enabled modes. Beacon enabled mode uses a slotted CSMA-CA channel access mechanism, where the backoff slots are aligned with the start of the beacon transmission. If a device wishes to transmit data frames or commands in each time slot, it waits for a random period time. If the channel is found to be busy, the device waits for a random period before trying to access the channel again. If

the channel is found to be idle, the device transmits its data after waiting the random backoff [18]. A backoff timer is initialized by using a random uniform distribution in the range $[0, 320 \cdot (2^{\text{BE}} - 1)] \mu\text{s}$ [16], where BE is backoff exponent. This beacon enabled mode is adopted in this paper.

A large number of energy efficient scheduling schemes have been proposed for wireless sensor networks in recent years [19–21]. In [19], the authors proposed a distributed queuing medium access control (MAC) scheme to guarantee the quality of service requirements of WBSNs. The authors of [20] proposed the cross-layer based battery-aware time division multiple access (TDMA) protocols for wireless monitoring networks in wireless healthcare applications. The main focus of [21] was a system level power consumption model associated with transmission distance and transmission data rate for WBSNs.

There are also a lot of work about spectral efficiency studies [22,23]. In [22], the authors developed a spectral-efficient multi-channel random wireless networks using stochastic geometry. This framework can maximize frequency utilization in both spatial and time domains. In [23], a virtual channel was introduced to increase the number of available channels by efficiently managing given spectral and temporal resources and therefore to further enhance the spectral efficiency.

Recently, the tradeoff between energy efficiency and spectral efficiency has attracted a lot of research interests, e.g., for IEEE 802.11 WLANs [24–26]. In contrast, little work has been considered for WBSNs. The previous works on WBSNs mainly focused on transmission schemes to minimize total power consumption and spectral efficiency separately, not considering their relationship.

On the basis of these factors stated above, energy consumption is a major concern in WBSNs, since battery-powered sensor nodes are expected to operate for a long time. Moreover, due to the scarcity of spectrum, efficient coexistence of IEEE802.15.4-based WBSNs in the ISM band is also a challenging problem. Unfortunately, energy efficiency and spectral efficiency are not always consistent and sometimes even conflict with each other. In most cases, it is possible to tradeoff energy efficiency and spectral efficiency in order to prolong the networks lifetime. Therefore, the performance of WBSNs coexistence based on the spatial distribution is studied in this paper, such as energy efficiency, area spectral efficiency, outage probability, and throughput. The tradeoff between energy efficiency and area spectral efficiency of WBSNs using the PPP model and the Matern hard-core point process (HCPP) with guard zone model is investigated and compared. In addition, transmit power is optimized to increase energy efficiency.

The contributions of this paper can be summarized as follows:

1) The tradeoff between energy efficiency and area spectral efficiency is analyzed in coexisting WBSNs. By using stochastic geometry, the feasible region and appropriate density are obtained when many WBSNs coexist in the same frequency channel.

2) The nearest neighbour distance power control scheme is proposed. The interference is caused seriously by the nearest neighbour node. Therefore, probability density function (PDF) of the transmit power is derived according to the nearest neighbour node distance. Simulation results show that it can enhance energy efficiency.

3) Using stochastic geometry, the guard zone size of every transmitting nodes is analyzed, which can naturally decrease the co-channel interference and increase the success probability. Furthermore, area spectral efficiency of coexisting WBSNs is analyzed under different guard zone sizes.

The remainder of this paper is organized as follows. The system model is introduced in Section 2. Section 3 formulates the power control, energy efficiency, area spectral efficiency of WBSNs using the PPP model. Section 4 describes energy efficiency and area spectral efficiency under the HCPP model. Section 5 illustrates and analyzes numerical results that show energy efficiency and area spectral efficiency tradeoff. Finally, concluding remarks are discussed in Section 6.

2 System model

The network model is regarded in this paper composed of multiple stationary WBSNs. The coexisting WBSNs locations are modeled as a isotropic Poisson cluster process coexisting in the \mathbb{R}^2 Euclidean space. The cluster process consists of the cluster center nodes (CNs) and cluster member sensor nodes (SNs)

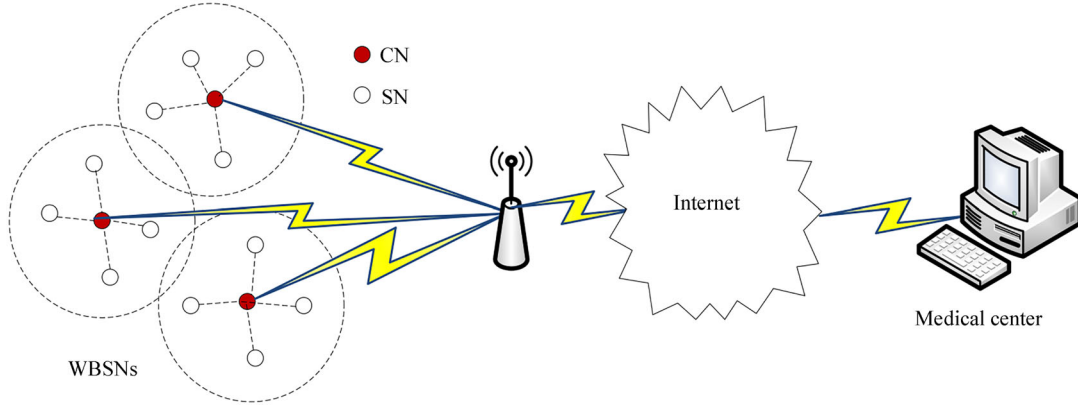


Figure 1 (Color online) Coexisting WBSNs.

such as in Figure 1. The CNs spatial distribution model is a PPP with intensity λ_{PPP} . For the Poisson cluster process, SNs are uniformly distributed around the CNs. The average number of SNs in each WBSNs is ω , then all the SNs in networks form a homogeneous PPP with intensity $\lambda_{\text{PPP}}\omega$. To simplify the analysis, it is assumed that each WBSNs will always have only one SN sending data at the same time. Therefore, each network is composed of a pair of SN and CN. The density of SNs can also be considered as λ_{PPP} . These many scattered small networks constitute the coexisting WBSNs. All nodes are assumed that they have identical physical layer characteristics and there is no statistical dependence at different nodes.

This PPP model is denoted by $\phi = \{(x_i, t_i, P_i)\}$, where

(1) $\phi = \{x_i\}$ denotes the location of the i -th SN in the \mathbb{R}^2 Euclidean space, ϕ is always assumed Poisson with positive and finite intensity λ_{PPP} .

(2) $\{t_i\}$ is a mark of node x_i , which denotes the backoff timer of CSMA/CA, uniformly distributed on $[0, 1]$ according to $[0, \text{backoff timer}/320 \cdot (2^{\text{BE}} - 1)]$, $\text{BE} \in [0, 5]$ [18].

(3) $\{P_i\}$ symbolizes the transmit power of node x_i .

The target domain of area is denoted as M . Denoting by k is the number of SNs in M . The number of points k has a Poisson distributed with mean $\lambda_{\text{PPP}}\hat{M}$, where \hat{M} is the standard Lebesgue measure of M . The probability of having k SNs in the domain M is expressed as [16]

$$P(\phi(M) = k) = \exp(-\lambda_{\text{PPP}}\hat{M}) \frac{(\lambda_{\text{PPP}}\hat{M})^k}{k!}. \quad (1)$$

For analysis, only path-loss attenuation effects are considered, additional channel effects are ignored such as shadowing and fast fading. In particular, if the transmit power is P_t and the path-loss exponent is α , the receive power at a distance r from the transmitter is given by $P_t h r^{-\alpha}$. The random variable h follows an exponential distribution with mean $1/u$, which is denoted as $h \sim \exp(u)$. In our model, contention domain is that node y is in the contention domain of node x if the power received by x from y is above some detection threshold. The neighbours of a node are the nodes in its contention domain. Let us define the contention domain as

$$C_x = \{(x_i, t_i, P_i) \in \phi : P_i h \|x_i - x_j\|^{-\alpha} \geq \gamma\}, \quad (2)$$

where γ is the detection threshold of signal to interference plus noise ratio (SINR), $\|\cdot\|$ denotes the Euclidean norm. Throughout this paper, the SN x_i is younger than the x_j (if $t_i < t_j$). The youngest SN, which has the lowest mark (the minimum backoff time), will first send data in this time slot according to CSMA/CA mechanism [27]. The node having the lowest mark in its protection domain is retained in HCPP model.

3 Energy efficiency and area spectral efficiency tradeoff in PPP model

3.1 SINR and outage probability

Without loss of generality, due to the stationary of the point process, considering the transmit node SN_0 is located at the origin, $\text{SN}_0 \in \phi$. The receiving node (CN) corresponding to it is located at (r, θ) , where r is the distance of $\text{CN} - \text{SN}_0$ and θ is the orientation. If $\tilde{\phi}_L$ denotes the contain domain, the cumulative interference I is caused by all other transmit nodes located in the contain domain ($x_i \in \tilde{\phi}_L$) of SN_0 . Measured at a origin point can be expressed as [16]

$$I = \sum_{x_i \in \tilde{\phi}_L} P_i h_i \|x_i\|^{-\alpha}, \quad (3)$$

where $x_i \in \tilde{\phi}_L$ denotes the set of all transmit nodes located in the contain domain, P_i is the transmit power of node x_i , h_i is fading coefficient, assumed to depend only on the distance, and $\|x_i\|$ is the distance of nodes x_i and the SN_0 . Hence, the SINR is given by

$$\text{SINR} = \frac{P_t h r^{-\alpha}}{W + I}, \quad (4)$$

where P_t is the transmit power of node SN_0 , I is the interference power given by (3) and W is noise power. In the presence of inter networks interference, outage occurs when the SINR of the receive node is below an acceptable threshold γ . The outage probability, which is the same as the cumulative distribution function (CDF) of the SINR, is expressed as

$$p_{\text{out}} = P\left(\frac{P_t h r^{-\alpha}}{W + I} \leq \gamma\right). \quad (5)$$

Lemma 1. The outage probability of a WBSNs in PPP model can be written as

$$p_{\text{out_ppp}} = 1 - \exp\left(-\frac{\gamma r^\alpha W}{P_t}\right) \exp\left(-\lambda_{\text{ppp}} \left(\frac{2\pi^2}{\alpha \sin(\frac{2\pi}{\alpha})}\right) \left(\frac{\gamma}{u}\right)^{2/\alpha} r^2\right). \quad (6)$$

Proof. See Appendix A.

3.2 Nearest neighbour distance power control

Effective transmit power control is a critical issue in the design and performance of WBSNs. On one hand, to avoid negative impact of electromagnetic radiation on human body reduces the interference caused to other nodes, it is critical to keep a low transmit power in WBSNs. On the other hand, choosing a lower transmit power can also impact the connectivity and performance of the network reliability. The transmit power should be changed and adjusted with different surroundings. The transmission success probability varies with the change of many WBSNs distribution density. Hence, the transmit power should possibly be adjusted according to the networks distribution density. One benefit to controlling the power level, particularly for battery-operated terminals, is to reduce energy consumption. The interest here, however, is to mitigate the interference of coexisting networks. Ref. [28] has examined the merits of the random power control. Tae-Suk Kim and Seong-Lyun Kim have concluded that the random power control can improve the connectivity of the network as the density of the network increases.

The interference is the main limiting performance factor in coexisting WBSNs. It depends strongly on the nearest neighbour node. The geographical positions of WBSNs are an important influencing factor in affecting the coexistence interference. For the reason that, the nearest neighbour distance distribution is the first consideration. The distance denoted by D from any node to its nearest neighbour. We change the power according to the nearest neighbour distance when the D is less than detection range, on the other hand, the random power control method of [28] is adopted. The nearest neighbour distance distribution can be expressed by [29]

$$f(D) = 2\pi\lambda_{\text{PPP}}D \exp(-\pi\lambda_{\text{PPP}}D^2). \quad (7)$$

The received power can be written as $P_r = P_t hr^\alpha$ [29]. Then, transmission is regarded successful if the received power $P_t hr^\alpha > \gamma$. The minimum transmission power can be got as much as possible to reduce interference with the nearest neighbour point. The probability density function of transmit power is obtained according the nearest neighbour distance distribution as follows:

$$f(p) = \begin{cases} \frac{2\pi\lambda_{\text{PPP}}}{\alpha} \left(\frac{ph}{\gamma}\right)^{\frac{2}{\alpha}-1} \exp(-\pi\lambda_{\text{PPP}}(\frac{ph}{\gamma})^{2/\alpha}), & r < D, \\ \frac{1}{p_{\text{max}} - p_{\text{min}}}, & r > D, \end{cases} \quad (p_{\text{min}} < p < p_{\text{max}}). \quad (8)$$

Proof. See Appendix B.

3.3 The tradeoff between energy efficiency and area spectral efficiency

3.3.1 Energy efficiency

An accurate and comprehensive energy efficiency model is the basis of power consumption analysis in energy efficient system design. The actual power efficiency is relatively small especially in low power consumption system. Therefore, the circuit power must be considered. In this paper, energy efficiency is defined as the ratio of the average number of transmitted bits to the average energy consumption with unit bps/Hz/W [30]

$$\eta = \frac{[\text{average number of transmitted bits}]}{[\text{average consumed energy}]}.$$

Let S_{PPP} be the normalized coexist networks throughput under PPP model, defined as the average time of successfully transmit payload bits. Then S_{PPP} can be written as $S_{\text{PPP}} = \lambda_{\text{PPP}}(1 - p_{\text{out-PPP}})L$, where L is the valid transmitted data packet length. The energy efficiency is given by

$$\eta_{\text{PPP}} = \frac{S_{\text{PPP}}}{(\xi P_t + P_c)T}. \quad (9)$$

In (9), $T = T_t + T_{\text{sense}} + T_{\text{back}} + T_{\text{idle}}$, where $T_t, T_{\text{sense}}, T_{\text{back}}, T_{\text{idle}}$ respectively denote the total time that the radio is in the transmitting, sensing channel, backoff time and idle time. The peak-to-average power ratio (PAPR) is defined as ξ , which is the peak amplitude squared (giving the peak power) divided by the root mean square. A 2450 MHz direct sequence spread spectrum (DSSS) physical layer (PHY) employs offset-quadrature phase shift key (O-QPSK) modulation with half sine pulse shaping. Therefore the PAPR is 1.4. The drain efficiency of the power amplifier (PA) is ζ . It is small less than 10%. Therefore, the circuit power must be considered. P_t is the transmit power. It is a key parameter to be designed in this paper. Circuit power, P_c , accounts for a large part of the input power. It is necessary to consider the circuit power in the energy efficiency.

3.3.2 Area spectral efficiency

In the past decade, several short range wireless technologies, for example, IEEE 802.15.4, WirelessHART, and ISA 100, have been developed for wireless sensor network (WSN). These technologies related to WSN primarily operate in the unlicensed ISM bands which are shared with other major wireless standards such as IEEE 802.11, Bluetooth, and cordless phone. With the growing proliferation of wireless devices and systems, the ISM bands are increasingly becoming congested and the coexistence issues are becoming more and more critical for the applications of WSN. As a branch of WSN, WBSNs are also faced with the same problem as mentioned above. Consequently how to maximize the spectrum utilization is a major concern [31].

There are 16 channels in the 2.4 GHz band, all of which are non-overlapping with each other. In order to utilize wireless channel resources efficiently, the spectral efficiency is analyzed. Area spectral efficiency performance metric was introduced in [32] to quantify the spectrum utilization efficiency of cellular

systems. In this paper, the concept of area spectral efficiency quantifies the spatial spectral utilization efficiency based on the definition of coexistence area. Specifically, area spectral efficiency is defined as the maximum average data rates per unit bandwidth per unit area supported with unit $\text{b/s}/(\text{Hz} \cdot \text{m}^2)$ [33]. The first objective is to minimize the total number of channels to decrease interferences to maximize the spectral efficiency [16]. According to the throughput, the area spectral efficiency is expressed as

$$\delta_{\text{PPP}} = \frac{S_{\text{PPP}}}{TB}, \quad (10)$$

where B denotes channel bandwidth.

3.3.3 The tradeoff between energy efficiency and area spectral efficiency

The energy efficiency and spatial frequency utilization are two important performance metrics for WBSNs coexistence. However, decreasing the consumed energy, equivalently maximizing the energy efficiency, and improving the area spectral efficiency are conflicting objectives [34]. Therefore, there should be a fundamental tradeoff between the energy efficiency and the spectral efficiency, i.e.,

$$\eta_{\text{PPP}} = f(\delta_{\text{PPP}}). \quad (11)$$

We take the derivation ($\frac{d(\eta_{\text{PPP}})}{d(\delta_{\text{PPP}})} = 0$) of equation (11), the δ_{PPP}^* is obtained, then get the optimal the λ_{PPP} when the energy efficiency is maximum.

In this section, the energy efficiency and area spectral efficiency tradeoff can be well approximated [22]. Energy efficiency and area spectral efficiency can achieve better values simultaneously under certain conditions. We will have the following optimization problem:

$$\arg \max \eta_{\text{PPP}}, \text{ s.t. } \delta_{\text{PPP}} = \text{constant}. \quad (12)$$

3.3.4 Tradeoff judgement coefficient analysis (TCA)

In this section, a new approach is presented to judge the energy efficiency and the area spectral efficiency metric, a new criterion based on the economic efficiency in [23]. To alleviate the problems with the existing relationship analysis approaches, a criteria is proposed in performing tradeoff analysis for finding a Pareto optimal alternative. The basic idea is to find a certain coefficient which can describe the energy efficiency or area spectral efficiency reaching the best balance. Specifically, a total economic maximization is formulated that allows for a flexible tradeoff between flow-level performance and power consumption[35]. Similar to [23], this criterion of judgement is proposed as a possible complementary measure to the energy efficiency and area spectral efficiency. By cooperatively considering both η_{PPP} and δ_{PPP} , the tradeoff criterion metric is defined as

$$C_{\text{TCA}} = \kappa_r(1 + \log_2(\kappa_e \eta_{\text{PPP}}) + \log_2(\kappa_s \delta_{\text{PPP}})) - \kappa_c P_{\text{total}}, \quad (13)$$

where $k_r = 5.9$ is the tradeoff ratio factor, $k_e = 2.9(\text{J}/\text{bit})$, $k_s = 1.4(\text{Hz} \cdot \text{m}^2/\text{s}/\text{bit})$ is the energy efficiency and area spectral efficiency scale parameter respectively. The factor $k_c = 1.2 \times 10^3(1/\text{J})$ is the energy cost per Joule. Here the parameter C_{TCA} is equivalent cost efficiency of cellular network. The main purpose of this estimate coefficient is to evaluate the performance metric for the relationship of energy and area spectral efficiency.

4 Energy efficiency and area spectral efficiency tradeoff in HCPP model

The CSMA-CA mechanism is widely employed in wireless networking due to its simplicity and performance efficiency [36]. CSMA guard zone is defined as the region around each node where interfering transmissions are inhibited. Some MAC protocols adopt smaller exclusion zones method to protect scheduled transmissions that nodes which are close by never transmit simultaneously [37]. Therefore, the HCPP model with different guard zones is further analyzed.

In this section, the effect of having guard zone and the size of guard zone are examined. In ad hoc and sensor networks, it is important that the distribution of the distances between the terminals be known [38]. In CSMA protocol, a node which needs to access the shared wireless medium senses its occupation and refrains from transmitting if the channel is already locally occupied. Hence, each active node has been set some exclusion region around itself preventing other nodes located in this region from transmitting [39]. According to stochastic geometry analysis, the success probability of networks is seriously affected by the guard zone size [40]. However, the performance of network will be reduced if the value of guard zone is too large. Therefore it is necessary to consider the impact of the protected area to the network.

First, the density of the HCPP model is calculated. Conditioned on the lowest mark t , the probability that node is selected equals to

$$P_{\text{hcpp}} = \int_0^1 \mathbb{E}[(1-t)^n] dt = \frac{1 - \exp(-\lambda_{\text{ppp}}\pi z^2)}{\lambda_{\text{ppp}}\pi z^2}. \quad (14)$$

Then the final density of the HCPP model with guard zone is expressed as

$$\lambda_{\text{hcpp}} = \lambda_{\text{ppp}} \frac{(1 - \exp(-\lambda_{\text{ppp}}\pi z^2))}{\lambda_{\text{ppp}}\pi z^2} = \frac{(1 - \exp(-\lambda_{\text{ppp}}\pi z^2))}{\pi z^2}, \quad (15)$$

where z is guard zone radius.

Proof. See Appendix C.

A minimum distance is imposed between the transmitters. For relatively a certain guard zone, it forms a hard-core point process. It can increase the successful transmissions probability, but it also reduces the throughput because the intensity is low. The outage probability of the HCPP model is written as

$$p_{\text{out_hcpp}} = 1 - \exp\left(-\frac{\gamma u r^\alpha W}{P_t}\right) \exp\left(-\lambda_{\text{hcpp}} d(\alpha) \left(\frac{\gamma}{u}\right)^{2/\alpha} r^2\right). \quad (16)$$

Proof. See Appendix D.

The performance of the tradeoff energy efficiency and area spectral efficiency in HCPP model is further studied. In HCPP model with guard zone, the size of guard zone is a very critical parameter which can affects highly the throughput. Therefore, there is a tradeoff between guard zone and the throughput. The optimal value of the guard zone can change the relationship of energy efficiency and area spectral efficiency. The energy efficiency, area spectral efficiency and their relationship in the HCPP model can be expressed according to PPP model as follows:

$$\eta_{\text{hcpp}} = \frac{\lambda_{\text{hcpp}}(1 - p_{\text{out_hcpp}})L}{\left(\frac{\xi}{\zeta} P_t + P_c\right)T}, \quad (17)$$

$$\delta_{\text{hcpp}} = \frac{\lambda_{\text{hcpp}}(1 - p_{\text{out_hcpp}})L}{TB}, \quad (18)$$

$$\eta_{\text{hcpp}} = g(\delta_{\text{hcpp}}). \quad (19)$$

5 Results and analysis

In this section, some numerical examples using Matlab are shown in order to substantiate the accuracy of the proposed analysis and to investigate the performance of the coexisting WBSNs. In the simulation, a coordinator and a transmitting sensor node form a star network. The initial maximum transmission distance between the coordinator and sensor node in a network is set to three meters. The radio settings are configured according to the IEEE 802.15.4 standard. In this study, an on-body path-loss model with an exponent of $\alpha = 3$. The basic of the simulation parameters are shown in Table 1.

Figure 2 is the PPP and HCPP model established via Monte Carlo simulations to verify the accuracy of WBSNs distribution. Many transmission nodes have scattered in the 20 m×20 m area according to a

Table 1 System parameters

Transmission power(mW)	0.1
On-body path-loss exponent	3
SINR threshold(dB)	-20
Circuit power(mW)	30
The peak-to-average ratio	1.4
The drain efficiency of the PA	0.08
The contain domain R(m)	5
Channel bandwidth(MHz)	2
Frequency (GHz)	2.4
Packet payload(bytes)	40

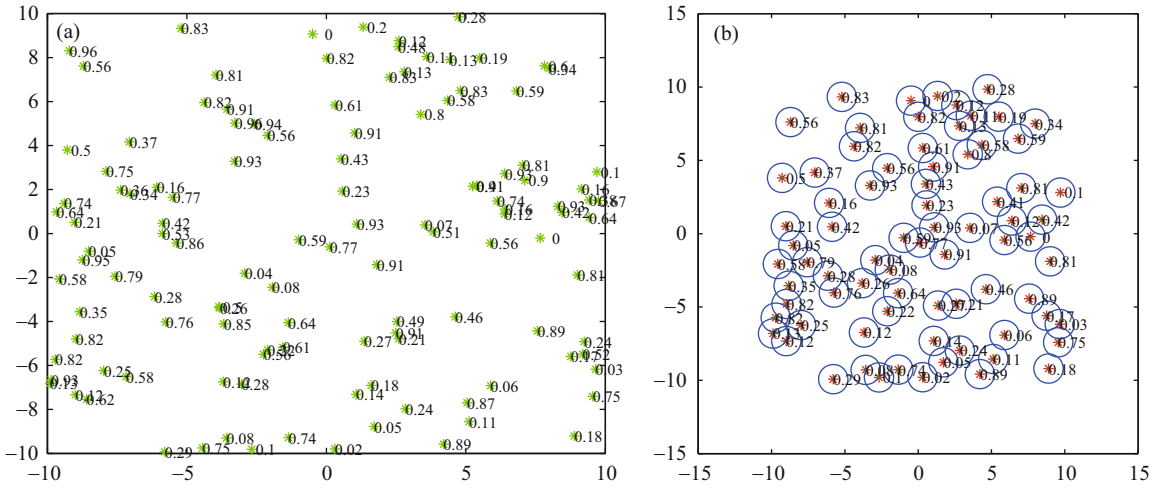


Figure 2 (Color online) (a) PPP model; (b) HCPP model.

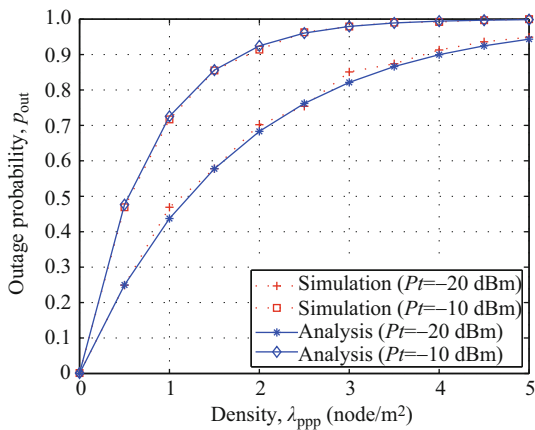


Figure 3 (Color online) Outage probability of the PPP model.

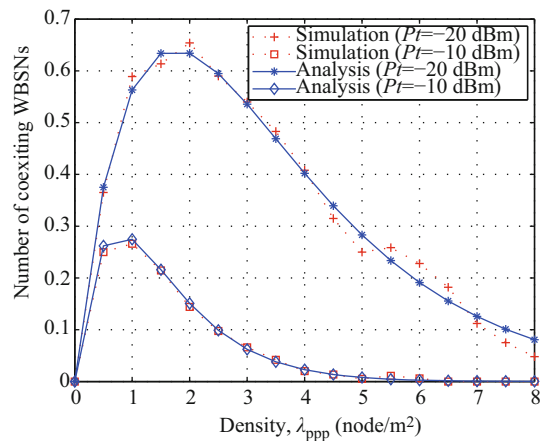


Figure 4 (Color online) The number of coexisting WBSNs.

certain density ($\lambda_{ppp} = 1$). In Figure 2(b) the protect domain around each node is set. If the closest node distribution distance is less than the value of guard zone, the node with the smallest mark is retained. Hence, the protected area around each node is formed.

Figure 3 illustrates how the outage probability of these networks change with various density for different transmission power. Figure 4 exhibits the number of coexisting WBSNs with the different transmission power. It is shown that adjusting the transmit power can improve the number of coexisting

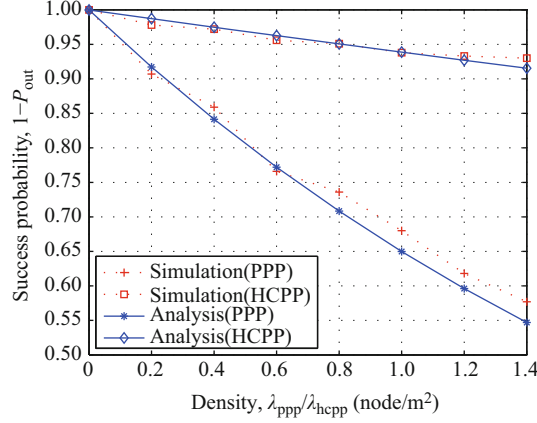


Figure 5 (Color online) Success probability of PPP and HCPP models.

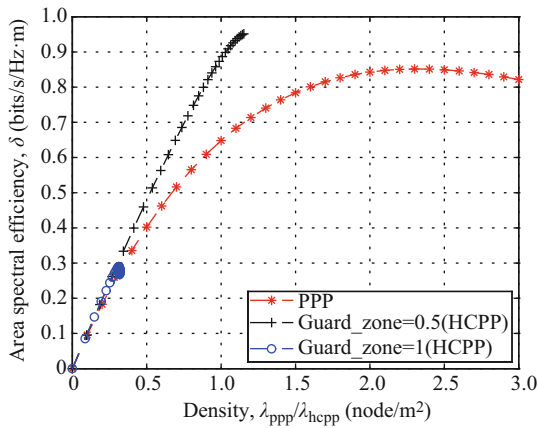


Figure 6 (Color online) Area spectral efficiency of PPP and HCPP models.

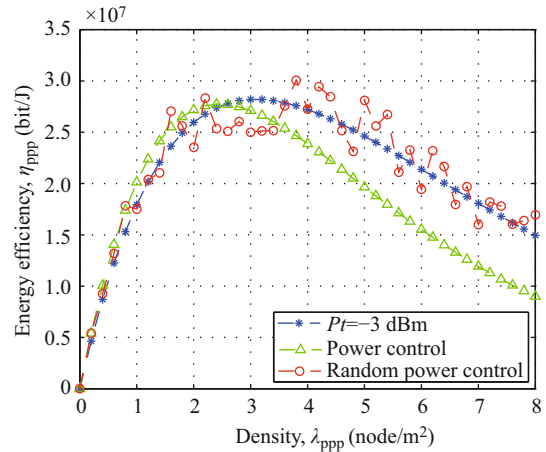


Figure 7 (Color online) Energy efficiency of two power control schemes.

transmitting nodes at the same time. The result is to increase the radius of the domain. Each curve represents a scenario with a certain power. It is also noted that the number of coexisting WBSNs of $P_t = -10$ dBm is about two times of $P_t = -20$ dBm, mainly because the outage probability is different.

The success probability in PPP and HCPP with guard zone $z = 0.5$ m is shown in Figure 5. The success probability of HCPP is always greater than 0.9. However, the PPP model declines rapidly as the density increases. This suggests that the HCPP with guard zone model naturally decreases the interference, but at the cost of inefficient spatial reuse as shown in Figure 6. In order to understand the effect of the guard zone, the area spectral efficiency is analyzed when the guard zone $z = 0.5$ m and $z = 1$ m. The area spectral efficiency decreases along with the guard zone increasing. The area spectral efficiency is better than the PPP model as $z = 0.5$ m. Therefore, the optimal guard zone can enhance the performance of coexisting networks.

The simulation results are listed in Figure 7 for the energy efficiency of two power control strategies vary at different density $\lambda_{ppp} = 1$. In this figure, $P_{min} = 0.01$ mW and the $P_{max} = 1$ mW are set. $P_t = 0.5$ mW is the intermediate value of and in order to more accurately compare the simulation results. The power control about the neighbour's distance is excellent to the constant power, this scheme is adopted when the density is relatively small. The energy efficiency performance for the random power control is better than the constant power on the whole because the points above line is more than the points below constant power line. So that is why we adopt this random power control when the intensity of coexistence networks is relatively large. More specifically, two different optimize schemes have been

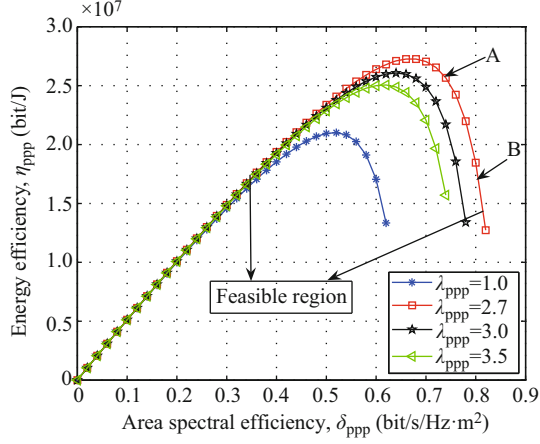


Figure 8 (Color online) The tradeoff between energy efficiency and area spectral efficiency of the PPP model.

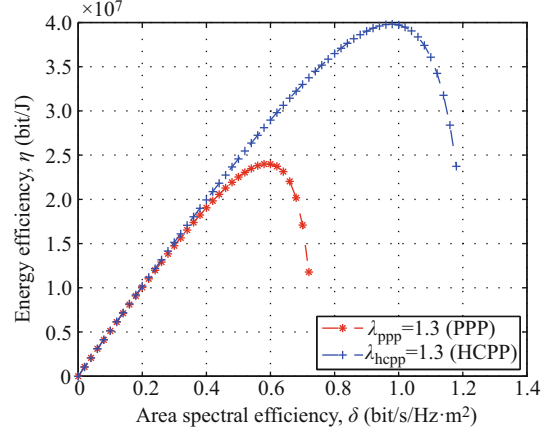


Figure 9 (Color online) The tradeoff of energy efficiency and area spectral efficiency of PPP and HCPCP models.

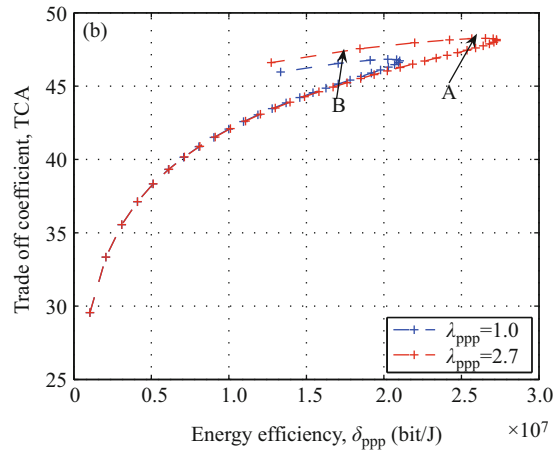
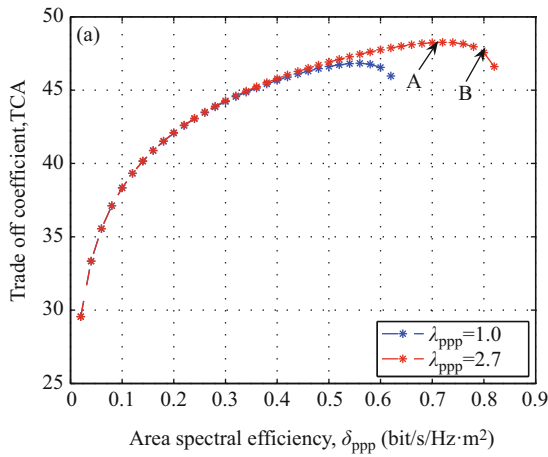


Figure 10 (Color online) (a) TCA-area spectral efficiency; (b) TCA-energy efficiency.

proposed to mitigate the power consumption to varying degrees, moreover, their complexity is lower than some of optimize schemes.

A tradeoff between energy efficiency and area spectral efficiency is presented in Figure 8. It proceeds to investigate the relationship of the energy efficiency and area spectral efficiency at various distribution density. It is shown that the energy efficiency η_{PPP} is concave with λ_{PPP} . The energy efficiency is monotonically increasing with the density λ_{PPP} less than about 2.7, then became decline. The maximum value in the Figure 8 is in the $\lambda_{\text{PPP}} = 2.7$ curve. There is no other line over it. This simulation result is consistent with the theory of optimization. However, as the number of nodes increases or decreases, the energy efficiency begins to decrease. The value is minimum when the $\lambda_{\text{PPP}} = 1$.

In Figure 9, the tradeoff of energy efficiency and area spectral efficiency metric under PPP and HCPCP model as the $\lambda_{\text{PPP}} = 1.3$ and $z = 0.5$ m are compared. Obviously the energy efficiency and area spectral efficiency of HCPCP achieve a better performance than PPP model. That is, the HCPCP with guard zone model decreases the interference clearly and increases the transmitting success probability, but at the cost of density of networks. The tradeoff judgement coefficient in Figure 10 is proposed as a possible complementary measure to the area spectral efficiency and energy efficiency performance metrics. Such as the curve, the dot A and B corresponding to the Figure 8. The Pareto optimal frontier can be indicated as the part on the tradeoff curve between the points A and B.

The area spectral efficiency and energy efficiency have been analyzed. Both the RF and the circuit power have also been considered in energy efficiency. Simulation results have shown that the density of

network is a key parameter to the coexisting networks. The performance is the best when the distribution $\lambda_{\text{PPP}} = 2.7$. That is to say, it would be better if the average distance is no less than $1/(2 \times \sqrt{2.7}) = 0.3$ m according to the average distance [41] between the closest people.

6 Conclusions

This paper has characterized the performance of coexisting IEEE 802.15.4-based WBSNs by outage probability, energy efficiency, and area spectral efficiency using the stochastic geometry tool. The fundamental tradeoff between energy efficiency and area spectral efficiency of WBSNs has been derived and compared under two different models. HCPP model forms a protected area whose points are never closer to each other than some given distance [39]. The guard zone method has also been adopted to mitigate the coexistence interference. Although the performance of HCPP model is better than the PPP model, the main drawback of the HCPP model is in its selection process. It does not permit any transmitters to be very close. The nodes distribution has not yet been considered. This particular thinning process can lead to the inaccuracy of performance analysis of the system [42]. The PPP model, however, does not change the networks distribution. It can ensure more practical results. In addition, the nearest neighbour distance power control strategy has been proposed. This strategy has been shown to be able to decrease the co-channel interference and enhance the energy efficiency. Feasible regions have been given for different densities of coexisting WBSNs. The results have also shown that the outage probability is one of the key performance metrics in coexisting WBSNs. The optimal density of coexisting WBSNs has been obtained as well. Future investigations include the testing and validating of the aforementioned achievements to the actual system.

Acknowledgements This work was supported by EPSRC TOUCAN Project (Grant No. EP/L020009/1), EU FP7 QUICK Project (Grant No. PIRSES-GA-2013-612652), EU H2020 ITN 5G Wireless Project (Grant No. 641985), National Natural Science Foundation of China (Grant Nos. 61210002, 61401256), MOST 863 Project in 5G (Grant No. 2014AA01A701), and International S&T Cooperation Program of China (Grant No. 2014DFA11640).

Conflict of interest The authors declare that they have no conflict of interest.

References

- 1 Yang G Z. *Body Sensor Networks*. London: Springer, 2006. 1–397
- 2 Pantelopoulos A, Bourbakis N G. A survey on wearable sensor-based systems for health monitoring and prognosis. *IEEE Trans on Syst*, 2010, 18: 1–12
- 3 Martelli F, Verdone R. Coexistence issues for wireless body area networks at 2.45 GHz. In: *Proceedings of European Wireless*, Poznan, 2012. 18–20
- 4 Deylami M, Jovanov E. Performance analysis of coexisting IEEE 802.15.4-based health monitoring WBSNs. In: *Proceedings of 34th Annual International Conference of the IEEE EMBS*, San Diego, 2012. 2464–2467
- 5 Wang L S, Goursaud C, Nikaiein N, et al. Cooperative scheduling for coexisting Body Area Networks. *IEEE Trans Wirel Commun*, 2012, 12: 123–133
- 6 ElSawy H, Hossain E, Haenggi M. Stochastic geometry for modeling, analysis, and design of multi-tier and cognitive cellular wireless networks: a survey. *IEEE Commun Surv Tut*, 2013, 15: 996–1019
- 7 Peng J L, Tang H, Hong P L, et al. Stochastic geometry analysis of energy efficiency in heterogeneous network with sleep control. *IEEE Wirel Commun Lett*, 2013, 2: 615–618
- 8 Cavallari R, Martelli F, Rosini R. A survey on wireless body area networks: technologies and design challenges. *IEEE Commun Surv Tut*, 2014, 16: 1635–1657
- 9 Williams B, Allen B, True H, et al. A real-time, mobile timed up and go system. In: *Proceedings of IEEE 12th International Conference on Wearable and Implantable Body Sensor Networks*, Cambridge, 2015. 9–12
- 10 Hata Y, Kobashi S, Kuramoto K, et al. Home care system for aging people confined to bed by detached sensor network. In: *Proceedings of IEEE Workshop on Robotic Intelligence In Informationally Structured Space (RiiSS)*, Paris, 2011. 1–6
- 11 Mitchell E, Ahmadi A, Richter C, et al. Automatically detecting asymmetric running using time and frequency domain features. In: *Proceedings of IEEE 12th International Conference on Wearable and Implantable Body Sensor Networks*, Cambridge, 2015. 1–6

- 12 IEEE Computer Society. IEEE 802.15.4 Standard, Part 15.4: Wireless Medium Access Control (MAC) and Physical Layer (PHY) Specifications for Low-Rate Wireless Personal Area Networks (LR-WPANs). IEEE Std 802.15.4-2006. 2006
- 13 IEEE Computer Society. IEEE Standard for Local and Metropolitan Area Networks Part 15.6: Wireless Body Area Networks. IEEE Std 802.15.6-2012. 2012
- 14 Bluetooth SIG. Specification of the Bluetooth System. Version 4.0. 2010
- 15 Park P, Marco D P, Soldati P, et al. In: Proceeding of 6th Interference Conference on Mobile Adhoc and Sensor Systems, Macau, 2009. 130–139
- 16 Hesham E, Ekram H, Sergio C. Spectrum-efficient multi-channel design for coexisting IEEE 802.15.4 networks: a stochastic geometry approach. *IEEE J Sel Area Commun*, 2014, 13: 1611–1624
- 17 Zhang C Q, Wang Y L, Liang Y Q, et al. An energy-efficient MAC protocol for medical emergency monitoring body sensor networks. *Sensors*, 2016, 16: 1–19
- 18 IEEE Computer Society. IEEE 802.15.4, Part 15.4: Wireless Medium Access Control (MAC) and Physical Layer (PHY) Specifications for Low-Rate Wireless Personal Area Networks (LR-WPANs). Revision of IEEE Std 802.15.4-2003. 2006
- 19 Otal B, Alonso L, Verikoukis C. Highly reliable energy-saving MAC for wireless body sensor networks in healthcare systems. *IEEE J Sel Area Commun*, 2009, 27: 553–565
- 20 Su H, Zhang X. Battery-dynamics driven TDMA MAC protocols for wireless body-area monitoring networks in healthcare applications. *IEEE J Sel Area Commun*, 2009, 27: 424–434
- 21 Kim T H, Ha J Y, Choi S. Improving spectral and temporal efficiency of collocated IEEE 802.15.4 LR-WPANs. *IEEE Trans Mobile Comput*, 2009, 8: 1596–1609
- 22 Hong X M, Jie Y, Wang C X, et al. Energy-spectral efficiency trade-off in virtual MIMO cellular systems. *IEEE J Sel Area Commun*, 2013, 31: 2128–2140
- 23 Ku I, Wang C X, Thompson J. Spectral-energy efficiency tradeoff in relay-aided cellular networks. *IEEE Trans Wirel Commun*, 2013, 12: 4970–4982
- 24 Ngo H Q, Larsson E G, Marzetta T L. Energy and spectral efficiency of very large multiuser MIMO Systems. *IEEE Trans Commun*, 2013, 61: 1436–1449
- 25 Yao Y W, Cai X D, Giannakis G B. On energy efficiency and optimum resource allocation of relay transmissions in the low-power regime. *IEEE Trans Wirel Commun*, 2005, 4: 2917–2927
- 26 Martelli F, Buratti C, Verdone R. Modeling query-based wireless CSMA networks through stochastic geometry. *IEEE Trans Veh Technol*, 2014, 63: 2876–2885
- 27 Shah-Mansouri H, Pakravan M R, Khalaj B H. Analytical modeling and performance analysis of flooding in CSMA-based wireless networks. *IEEE Trans Veh Technol*, 2011, 60: 664–679
- 28 Kim T S, Kim S L. Random power control in wireless Ad Hoc networks. *IEEE Commun Lett*, 2005, 9: 1046–1048
- 29 Zhang X C, Haenggi M. Random power control in Poisson networks. *IEEE Trans Commun*, 2012, 60: 2602–2611
- 30 Pei Y Y, Liang Y C, eh K C, et al. Energy-efficient design of sequential channel sensing in cognitive radio networks: optimal sensing strategy, power allocation. *IEEE J Sel Area Commun*, 2011, 29: 1648–1659
- 31 Tang S S, Zhang Y, Zhang L Q, et al. Spectrum-efficient wireless sensor networks. *Int J Distrib Sens N*, 2015, 11: 1–2
- 32 Alouini M S, Goldsmith A J. Area spectral efficiency of cellular mobile radio systems. *IEEE Trans Veh Technol*, 1999, 48: 1047–1066
- 33 Zhang L, Yang H C, Hasna M O. Generalized area spectral efficiency: an effective performance metric for green wireless communications. *IEEE Trans Commun*, 2014, 62: 5367–5380
- 34 Akhtman J, Hanzo L. Power versus bandwidth efficiency in wireless communications: the economic perspective. In: Proceedings of IEEE 70th hicular Technology Conference-Fall, Alaska, 2009. 1–5
- 35 Guo W, OFarrell T. Capacity-energy-cost tradeoff in small cell networks. In: Proceedings of IEEE 75th hicular Technology Conference-Spring, Yokohama, 2012. 1–5
- 36 Ha J Y, Kim T H, Park H S, et al. An enhanced CSMA-CA algorithm for IEEE 802.15.4 LR-WPANs. *IEEE Commun Lett*, 2007, 11: 461–463
- 37 Baccelli F, Blaszczyszyn B. *Stochastic Geometry and Wireless Networks, Volume II: Applications*. Paris: Now Press, 2005. 68–88
- 38 Sousa E S, Silvester J. Optimum transmission ranges in a direct- sequence spread-spectrum multihop packet radio network. *IEEE J Sel Area Commun*, 1990, 8: 762–771
- 39 Hasan A, Andrews J G. The guard zone in wireless Ad hoc networks. *IEEE Trans Wirel Commun*, 2007, 6: 897–906
- 40 Haenggi M, On distances in uniformly random networks. *IEEE Trans Inf Theory*, 2005, 51: 3584–3586
- 41 Chiu S N, Stoyan D, Kendall W S, et al. *Stochastic Geometry and Its Applications*. 3rd ed. UK: Wiley Press, 2013. 35–55
- 42 Busson A, Chelius G, Gorce J. *Interference Modeling in CSMA Multi-Hop Wireless Networks*. Research Report–6624, INRIA. 2009

Appendix A Derivation of (6)

The outage probability of PPP model can be written as

$$p_{\text{out-PPP}} = P\left(\frac{P_t h r^{-\alpha}}{W + I} \leq \gamma\right)$$

$$\begin{aligned}
 &= 1 - \left(h \geq \left(\frac{\gamma r^\alpha (W + I)}{P_t} \right) \right) \\
 &= 1 - \left(\exp \left(-\frac{\gamma u r^\alpha (W + I)}{P_t} \right) \right) \\
 &= 1 - \exp \left(-\frac{\gamma u r^\alpha W}{P_t} \right) \exp \left(-\frac{\gamma u r^\alpha I}{P_t} \right) \\
 &= 1 - \exp \left(-\frac{\gamma u r^\alpha W}{P_t} \right) \mathcal{L}(s) \Big|_{s=\frac{\gamma u r^\alpha}{P_t}}. \tag{A1}
 \end{aligned}$$

Here, \mathcal{L} is the aggregate interference experienced by the test receiver node. We now evaluate the Laplace transform of interference $\mathcal{L}_{\text{PPP}}(\cdot)$

$$\mathcal{L}_{\text{PPP}}(s) \stackrel{(a)}{=} \left(1 + \frac{s}{u} \right)^{-1}, \tag{A2}$$

$$\begin{aligned}
 \mathcal{L}_{\text{PPP}}(s) &= E \left(\exp \left(-s \sum_{x \in \phi_{\mathcal{L}}} P_t h_i \|x_i\|^{-\alpha} \right) \right) \\
 &= E \prod_{x \in \phi_{\mathcal{L}}} \exp \left(-s P_t h_i \|x_i\|^{-\alpha} \right) \\
 &= E \prod_{x \in \phi_{\mathcal{L}}} \frac{1}{1 + \frac{s}{u} P_t h_i \|x_i\|^{-\alpha}}, \tag{A3}
 \end{aligned}$$

where (a) is written by the Laplace transform of the PDF of the channel gains.

$$E \prod_{x \in \phi_{\mathcal{L}}} f(x) \stackrel{(b)}{=} \exp \left(-\lambda \int_{R^2} (1 - f(x)) dx \right), \tag{A4}$$

$$\begin{aligned}
 \mathcal{L}_{\text{PPP}}(s) &= \exp \left(-\lambda_{\text{PPP}} \int_{R^2} \left(1 - \frac{1}{1 + \frac{s}{u} P_t \|x_i\|^{-\alpha}} dx \right) \right) \\
 &= \exp \left(-\lambda_{\text{PPP}} \int_{R^2} \frac{1}{1 + \left(\frac{s}{u} P_t \right)^{-1} \|x_i\|^\alpha} dx \right) \\
 &= \exp \left(-\lambda_{\text{PPP}} \left(\frac{2\pi^2}{\alpha \sin \left(\frac{2\pi}{\alpha} \right)} \right) \left(\frac{\gamma}{u} \right)^{2/\alpha} r^2 \right), \tag{A5}
 \end{aligned}$$

where (b) is obtained by using the Probability generating functional (PGFL) of a PPP [41]. It follows that $p_{\text{out_PPP}}$ in (6) can be obtained as follows:

$$p_{\text{out_PPP}} = 1 - \exp \left(-\frac{\gamma r^\alpha W}{P_t} \right) \exp \left(-\lambda_{\text{PPP}} \left(\frac{2\pi^2}{\alpha \sin \left(\frac{2\pi}{\alpha} \right)} \right) \left(\frac{\gamma}{u} \right)^{2/\alpha} r^2 \right). \tag{A6}$$

Appendix B Derivation of (8)

The received power is $P_r = P_t h r^{-\alpha}$. A transmission is regarded as successful if $P_r > \gamma$. So, $P_t h r^{-\alpha} > \gamma$.

$$P h r^{-\alpha} > \gamma \Rightarrow P = \frac{\gamma r^\alpha}{h} \Rightarrow r = \left(\frac{p h}{\gamma} \right)^{1/\alpha}, \tag{B1}$$

$$F_P(p) = P(P \leq p) = P \left(\frac{\gamma r^\alpha}{h} \leq p \right), \tag{B2}$$

$$\begin{aligned}
 f(p) &= 2\pi\lambda \left(\frac{p h}{\gamma} \right)^{1/\alpha} \exp \left(-\pi\lambda \left(\frac{p h}{\gamma} \right)^{2/\alpha} \right) \left| \frac{1}{\alpha} \left(\frac{p h}{\gamma} \right)^{\left(\frac{1}{\alpha} - 1 \right)} \right| \\
 &= \frac{2}{\alpha} \pi\lambda \left(\frac{p h}{\gamma} \right)^{\frac{2}{\alpha} - 1} \exp \left(-\pi\lambda \left(\frac{p h}{\gamma} \right)^{2/\alpha} \right). \tag{B3}
 \end{aligned}$$

Appendix C Derivation of (15)

Conditioned on t , the probability that x is selected can be expressed as

$$P_{\text{hcpp}} = \int_0^1 E[(1-t)^n] dt$$

$$\begin{aligned}
 &= \sum_{k=0}^{k=\infty} \int_0^1 (1-t)^k \frac{(\lambda_{\text{PPP}} \pi z^2)^k e^{-\lambda_{\text{PPP}} \pi z^2}}{k!} dt \\
 &= \sum_{k=0}^{k=\infty} \frac{(\lambda_{\text{PPP}} \pi z^2)^k e^{-\lambda_{\text{PPP}} \pi z^2}}{k!} \int_0^1 (1-t)^k dt \\
 &= \sum_{k=0}^{k=\infty} \frac{(\lambda_{\text{PPP}} \pi z^2)^k e^{-\lambda_{\text{PPP}} \pi z^2}}{k!} \frac{1}{k+1} \\
 &= \left(e^{\lambda_{\text{PPP}} \pi z^2} - 1 \right) \frac{e^{-\lambda_{\text{PPP}} \pi z^2}}{\lambda_{\text{PPP}} \pi z^2} \\
 &= \frac{\left(1 - e^{-\lambda_{\text{PPP}} \pi z^2} \right)}{\lambda_{\text{PPP}} \pi z^2}.
 \end{aligned}$$

Then,

$$\lambda_{\text{HCPP}} = \lambda_{\text{PPP}} P_{\text{HCPP}} = \frac{\left(1 - e^{-\lambda_{\text{PPP}} \pi z^2} \right)}{\pi z^2}. \tag{C1}$$

Appendix D Derivation of (16)

According to the outage probability of PPP model, we can express the outage probability of HCPP model $p_{\text{out,HCPP}}$ as

$$\begin{aligned}
 \mathcal{L}_{\text{HCPP}}(s) &= \exp \left(-\lambda_{\text{HCPP}} \int_{x_i \in \phi \setminus \{z\}} \left(1 - \frac{1}{1 + \frac{s}{u} P_t |x_i|^{-\alpha}} dx \right) \right) \\
 &= \exp \left(-\lambda_{\text{HCPP}} \int_{x_i \in \phi \setminus \{z\}} \frac{1}{1 + \left(\frac{s}{u} P_t \right)^{-1} |x_i|^\alpha} dx \right) \\
 &= \exp \left(-\lambda_{\text{HCPP}} \int_0^{2\pi} \int_z^\infty \frac{1}{1 + \left(\frac{s}{u} P_t \right)^{-1} r_i^\alpha} r dr \right) \Big|_{s=\frac{\gamma \mu r^\alpha}{P_t}}, \tag{D1}
 \end{aligned}$$

$$y = \left(\frac{s}{u} P_t \right)^{-1/\alpha} x = (\gamma r^\alpha)^{-1/\alpha}, \tag{D2}$$

$$d(y) = \frac{1}{\sqrt{3}} \arctan \frac{2y-1}{\sqrt{3}} - \frac{1}{6} \ln \frac{(1+y)^2}{1-y+y^2}, \tag{D3}$$

$$d(\alpha = 3) = d(y) \Big|_{\frac{(\gamma)^{-1/3}}{r} z}^\infty, \tag{D4}$$

$$\mathcal{L}_{\text{HCPP}}(s) = \exp \left(-\lambda_{\text{HCPP}} \left(\frac{s}{u} P_t \right)^{2/\alpha} d(\alpha) \right). \tag{D5}$$

Hence, the outage probability of HCPP model can be written as shown in (16).